

# Effects of Biaxial Loading on Inclined Surface Cracks Behavior

V.N. Shlyannikov, A.V. Tumanov, S.Yu. Kislova

Research Center for Power Engineering Problems of the Russian Academy of Sciences, Lobachevsky Street, 2/31, post-box 190, 420111, Kazan, RUSSIA; shlyannikov@mail.ru

**ABSTRACT.** *The elastic-plastic mixed mode parameters and stress intensity factors are obtained for surface cracks in a plate subjected to remote biaxial loading. Effect of load biaxiality combined with inclination angle on elastic-plastic both radial and angular stress distributions along the crack front of surface flow are investigated. Attention is paid on the strong variations of the nonlinear stress gradients near the border of a semi-elliptical surface crack. Based on the computed mixed mode stress fields, crack propagation angles along the inclined crack front are also determined. It is shown that the elastic-plastic radial and angular dimensionless stress fields and mode mixity parameters behaviour along crack front are more sensitive to load biaxiality than surface flaw geometries.*

## INTRODUCTION

It is well known that the mixed-mode conditions appear when the direction of the applied loading does not coincide with the orthogonal  $K_I$ - $K_{II}$ - $K_{III}$  space. In general, in the industrial practice the mixed-mode fracture and the mixed-mode crack growth are more likely to be considered the rule than the exception. The main feature of the mixed-mode fracture is that the crack growth would no longer take place in a self-similar manner and does not follow a universal trajectory that is it will grow on a curvilinear path. Despite of numerous elastic-plastic finite element analyses and experimental investigations of 2D-mixed mode crack extension problems, the understanding of both physics and mechanics of 3D-mixed-mode fracture phenomena is far from complete. Only few works related to 3D-analysis of fracture criteria and parameters behavior have been presented in literature [1-6].

Surface flaws are typical damages of different types of engineering structures. The assessment of both the form and size changes of the surface crack during propagation is an essential element for structural integrity prediction of such biaxially loaded engineering structures as the pressured vessels and pipelines in the presence of initial and accumulated operation damages. Often times in practice, inclined cracks can be encountered and accurate assessment of fracture resistance under monotonic loading or remaining fatigue life for such problems requires accounting for the geometry induced mode mixity, i.e., non-normal crack to the loading direction. Therefore three-

dimensional solutions obtained for biaxially loaded plates containing inclined surface flaws can generally be very useful in assessing the fracture conditions in the problem of interest.

In this present paper, extensive 3D finite element analysis are carried out to determine the elastic-plastic stress fields along the front of the inclined semi-elliptical surface cracks in plate subjected to remote normal biaxial tractions. Based on these results, the mode mixity parameters accounting for all three fracture modes are introduced. The strain energy density parameter is used to determine the fracture angle behavior along the crack front for inclined semi-elliptical surface flaws in plates under different biaxial loading conditions.

### NUMERICAL STRESS FIELD ANALYSIS

Fig. 1 illustrates an inclined semi-elliptical surface crack in a plate loaded by uniform biaxial loads. In this figure  $a$  is the crack depth in the plate thickness direction and  $2c$  is the crack length in the plate width/height direction and is measured in the inclined crack plane  $A-A$ . The crack front location or the parametric angle  $\phi$  of a semi-ellipse, goes from  $0^\circ$  to  $180^\circ$  in the plots for this surface flaw type and is measured from upper free surface, i.e.  $\phi = 0^\circ$ . Load biaxiality is given by ratio of the nominal stresses  $\eta = \sigma_{xx}^n / \sigma_{yy}^n$ . Different degrees of mixed mode are given by the combinations of crack plane position angle  $\alpha$  and load biaxiality  $\eta$ .

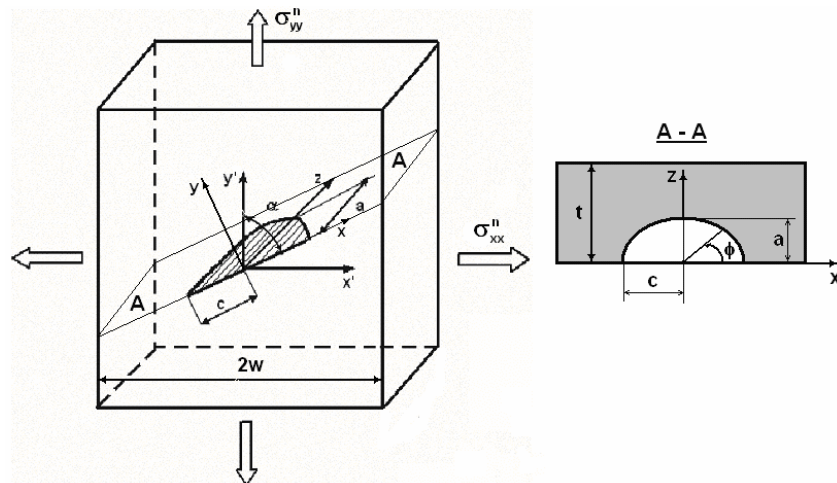


Figure 1. A semi-elliptical inclined surface crack in a plate under biaxial loading

Surface flaw in Fig.1 undergoes mixed mode fracture conditions having all three components of stress intensity factors, i.e. mode I, mode II and mode III. Although the remote loading is normal pressure loads, non-normal orientation of the crack to the loading direction causes the mode mixity.

The finite element analyses are performed using ANSYS [7] with 20-nodes isoparametric three-dimensional solid elements. Geometries considered are both semi-

circular and semi-elliptical surface cracks with aspect ratios of  $a/c=1.0$  and  $a/c=0.5$ , respectively. Biaxial tension and compression loadings with biaxial ratios of  $-1$ ,  $0$  and  $0.5$  are considered. The Ramberg-Osgood model was employed to define the stress-strain curve corresponding to the elastic-plastic material properties. Numerical results are presented for a hardening material characterized by the strain hardening exponent  $n = 3.96$ , the yield stress  $\sigma_0 = 460$  MPa, the Young's modulus  $E=200$  GPa, Poisson's ratio  $\nu=0.3$ .

Figs.2-3 show the typical numerical results of the normalized elastic-plastic angular stress distributions as a function of the crack front location parametric angle  $\phi$  and the crack inclination angle  $\alpha$  for surface flaw with aspect ratio of  $a/c=0.5$ . In these figures  $\theta$  is polar angle which varied from the lower to the upper crack surfaces. The results of angular stress distributions for general FEM-numerical solutions are normalized so that

$$\tilde{\sigma}_{e,\max}^{FEM} = \left( \frac{3}{2} s_{ij}^{FEM} s_{ij}^{FEM} \right)_{\max}^{1/2} = 1 \quad (1)$$

where  $\tilde{\sigma}_e$  and  $s_{ij}$  are equivalent and deviatoric stresses, respectively.

Fig. 2 depicts the dimensionless tangential stress distributions under equi-biaxial tension-compression with biaxial stress ratio  $\eta = -1$ . As can be seen in Fig.2a, the tangential stress  $\tilde{\sigma}_{\theta\theta}$ , is maximum at  $\theta = 0^\circ$  along the whole crack front when the surface crack is not inclined, i.e.,  $\alpha = 90^\circ$ . For mixed mode fracture conditions characterized by  $\eta = -1$  and  $\alpha = 45^\circ$  (Fig.2b), the tangential stress  $\tilde{\sigma}_{\theta\theta}$  continuously decreases with decreasing the crack front position angle  $\phi$  for a given combination of load biaxiality and inclination angle. The first observation that can be made is for each inclination angle, at the intersection of the crack front and the free surface the singularity of crack tip stress fields for  $0 \leq 2\phi/\pi \leq 0.2$  does not described by the HRR-model to enforce of the border effects.

Displayed in Fig.2c and 2d are the variations of the angular dimensionless tangential stress distributions under equi-biaxial tension-compression ( $\eta = -1$ ) as a function inclination angle  $\alpha$  for two main point of the crack front, i.e. at the free surface  $\phi = 0^\circ$  and at the deepest point  $\phi = 90^\circ$ . Fig. 2d shows that in the deepest point of the semi-elliptical crack front take place the symmetry of the angular tangential stress distributions  $\tilde{\sigma}_{\theta\theta}$  for whole range of the crack inclination angle variation. It should be noted that in the deepest point of the crack front at crack inclination angle of  $\alpha = 45^\circ$  the tangential stresses are equal to zero for any  $\theta$ . As it follows from Fig. 2c, at the same time on the free surface at  $\phi = 0^\circ$  the  $\tilde{\sigma}_{\theta\theta}$ -distributions are varied from the symmetrical type (like pure mode I for  $\alpha = 90^\circ$ ) to the anti-symmetrical type (like pure mode II for  $\alpha = 45^\circ$ ). Fig. 3 represents the angular distributions of the in-plane shear stress  $\tilde{\sigma}_{\rho\theta}$  and the out-of-plane shear stress  $\tilde{\sigma}_{\omega\theta}$  as a function of the crack front location  $\phi$  for the crack inclination angle  $\alpha = 45^\circ$  under equi-biaxial tension-compression  $\eta = -1$ . The results

indicate that due to the mode mixity of surface semi-elliptical crack, at the same biaxial loading conditions on the free surface of  $\phi = 0^\circ$  the in-plane shear stress  $\tilde{\sigma}_{\rho\theta}$  is maximum and the out-of-plane shear stress  $\tilde{\sigma}_{\omega\theta}$  is zero as this case represents pure mode II conditions, while in the deepest point of the crack front of  $\phi = 90^\circ$ , on the contrary,  $\tilde{\sigma}_{\rho\theta}$  takes a value of zero and  $\tilde{\sigma}_{\omega\theta}$  reaches its maximum that related to pure mode III.

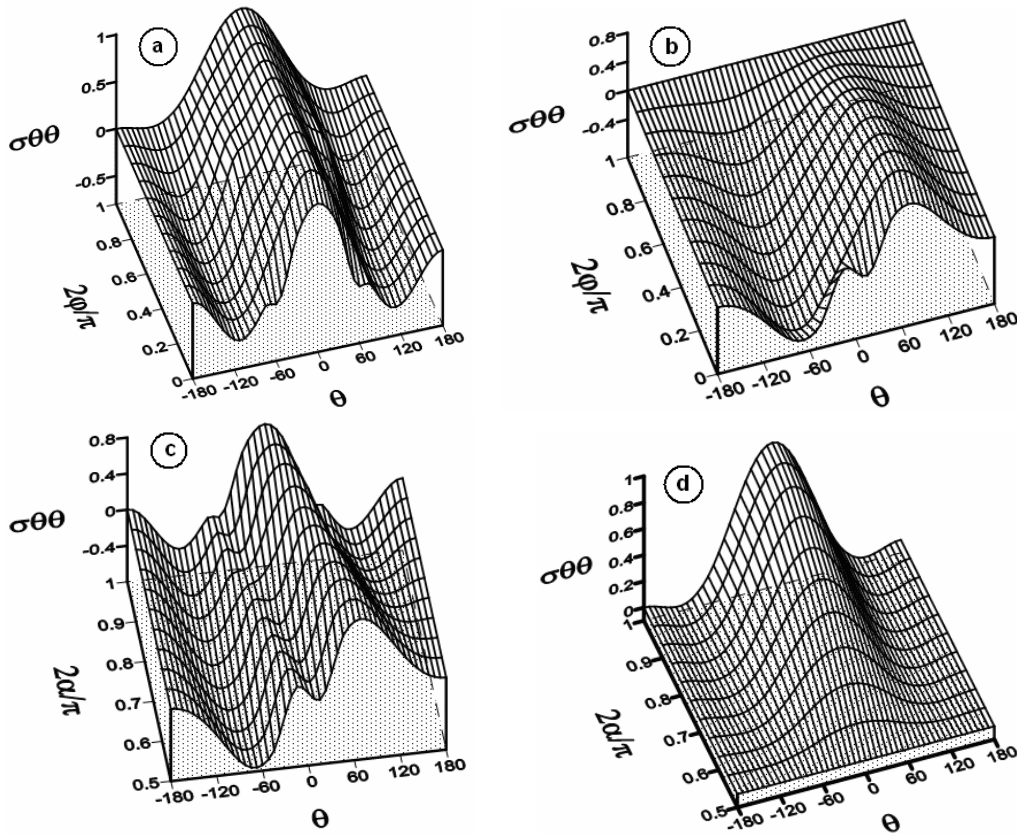


Figure 2. Angular tangential stress distributions under equi-biaxial tension-compression

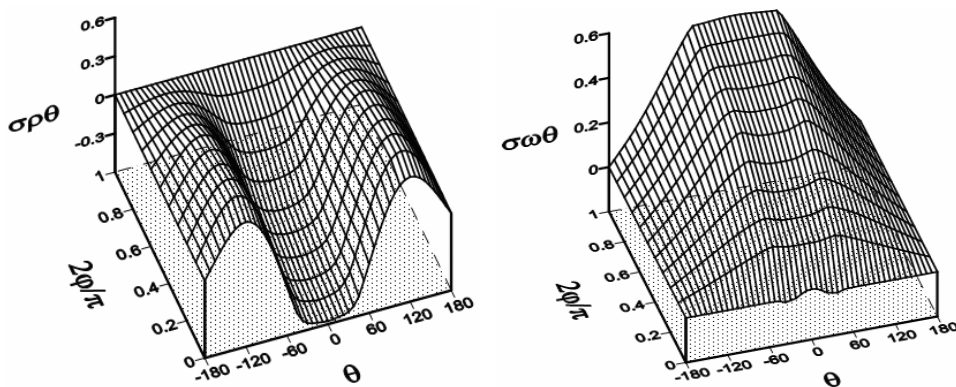


Figure 3. In-plane and out-of-plane shear stress angular distributions

## MODE MIXITY PARAMETERS DETERMINATION

Based on the numerical results for the angular stress component distributions along the inclined surface crack front under different load biaxiality, the values of both elastic and plastic mode mixity parameters have been determined for the semi-circular and semi-elliptical surface flaws.

The plastic mode mixity parameters were introduced as ratios between corresponding elastic-plastic stress components in the following form

$$M_{12} = \frac{2}{\pi} \operatorname{arctg} \left| \frac{\bar{\sigma}_{\theta\theta}}{\bar{\sigma}_{\rho\theta}} \right|, \quad M_{23} = \frac{2}{\pi} \operatorname{arctg} \left| \frac{\bar{\sigma}_{\omega\theta}}{\bar{\sigma}_{\rho\theta}} \right|, \quad M_{31} = \frac{2}{\pi} \operatorname{arctg} \left| \frac{\bar{\sigma}_{\omega\theta}}{\bar{\sigma}_{\theta\theta}} \right|. \quad (2)$$

In the case of elasticity the mode mixity parameters are described by equations

$$M_{12} = \frac{2}{\pi} \operatorname{arctg} \left| \frac{\bar{K}_I}{\bar{K}_{II}} \right|, \quad M_{23} = \frac{2}{\pi} \operatorname{arctg} \left| \frac{\bar{K}_{III}}{\bar{K}_{II}} \right|, \quad M_{31} = \frac{2}{\pi} \operatorname{arctg} \left| \frac{\bar{K}_{III}}{\bar{K}_I} \right|. \quad (3)$$

The elastic stress intensity factors for modes I, II and III of surface semi-elliptical crack were calculated from general equation

$$K_i = \sigma_i^\infty \sqrt{\pi \cdot l} \cdot f(\alpha, \phi, \eta), \quad \text{where } l = \frac{a}{\sqrt{\varepsilon^2 \cos^2 \phi + \sin^2 \phi}} \quad (4)$$

and remote stresses related to the nominal biaxial stress  $\sigma_{yy}^n$  ( $\eta = \sigma_{xx}^n / \sigma_{yy}^n$ ) defined as

$$\sigma_I^\infty = \sigma_{yy}^n (\cos^2 \alpha + \eta \sin^2 \alpha), \quad \sigma_{II}^\infty = \sigma_{yy}^n \frac{1-\eta}{2} \sin 2\alpha \cos \phi, \quad \sigma_{III}^\infty = \sigma_{yy}^n \frac{1-\eta}{4} \sin 2\alpha \sin \phi.$$

Fig.4 illustrates the elastic mode mixity parameters behavior as a function of the crack front position and the inclination angle of semi-elliptical surface crack ( $a/c=0.5$ ) under biaxial tension ( $\eta = 0.5$ ) and tension-compression ( $\eta = -1$ ). As it follows from results presented in Figs. 4, all fracture modes are encountered along the crack front when inclined surface crack is subjected to remote uniform biaxial loading different intensity. Moreover, the elastic mode mixity parameters like  $K_I/K_{II}$ ,  $K_{II}/K_{III}$  and  $K_I/K_{III}$ , does not remain constant along the curvilinear crack front of the surface flaw. Results for the plastic mode mixity parameters distributions under biaxial loading as a function of the crack front location and the inclination angle show similar trends.

## CRACK GROWTH DIRECTION ANGLE PREDICTION

Criterion of the inclined semi-elliptical crack growth direction prediction is elaborated on the basis of the strain energy density (SED) theory [8]. The expansion of the strain energy density field is resulting for inclined surface semi-elliptical crack subjected to biaxial loading:

$$\frac{dW}{dV} = \frac{(a_{11}K_I^2 + a_{12}K_I K_{II} + a_{22}K_{II}^2 + a_{33}K_{III}^2)}{4G\pi r} + \frac{(b_{11}K_I + b_{22}K_{II})}{2G\sqrt{2\pi r}} + \frac{T(1-\eta)\sigma}{16G} c_T, \quad (5)$$

where  $T = \sigma(1-\eta)\cos 2\alpha$  is the non-singular term.

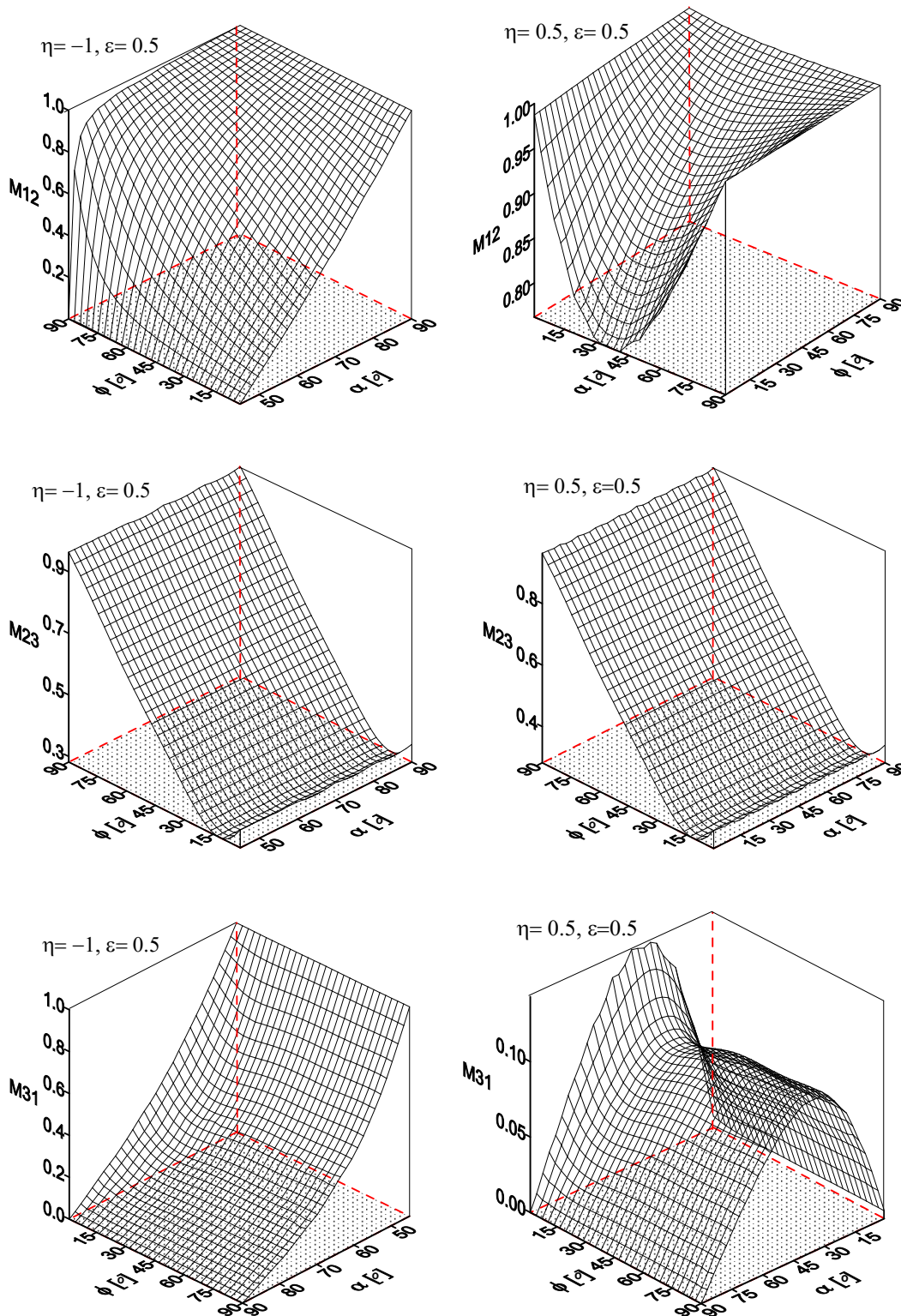


Figure 4. Mode mixity parameters behavior for semi-elliptical crack

The plastic strain energy density is obtained on the basis of the 3D-numerical results for different biaxial loading of the inclined surface crack in the following form

$$\left(\frac{dW}{dV}\right) = \int_0^{\varepsilon_{ij}} \sigma_{ij} d\varepsilon_{ij} = \frac{\sigma_0^2}{E} \left[ \frac{1+\nu}{3} \bar{\sigma}_e^2 + \frac{1-2\nu}{6} \bar{\sigma}_m^2 + \frac{\alpha n}{n+1} \bar{\sigma}_e^{n+1} \right], \quad (6)$$

where  $\bar{\sigma}_m$  is the normalized mean stress,  $\nu$  being the Poisson's ratio.

In the present work the third hypothesis of SED-criterion is used to determine the angle of crack propagation  $\theta^*$ . Thus, a line drawn from each point on the crack front in the normal plane at the angle  $\theta^*$  with respect to the crack plane indicates the directions in which the strain energy density has its extreme value  $\left. \frac{\partial \bar{W}}{\partial \theta} \right|_{r=r_c} = 0$ ,  $\bar{W} = dW/dV$ .

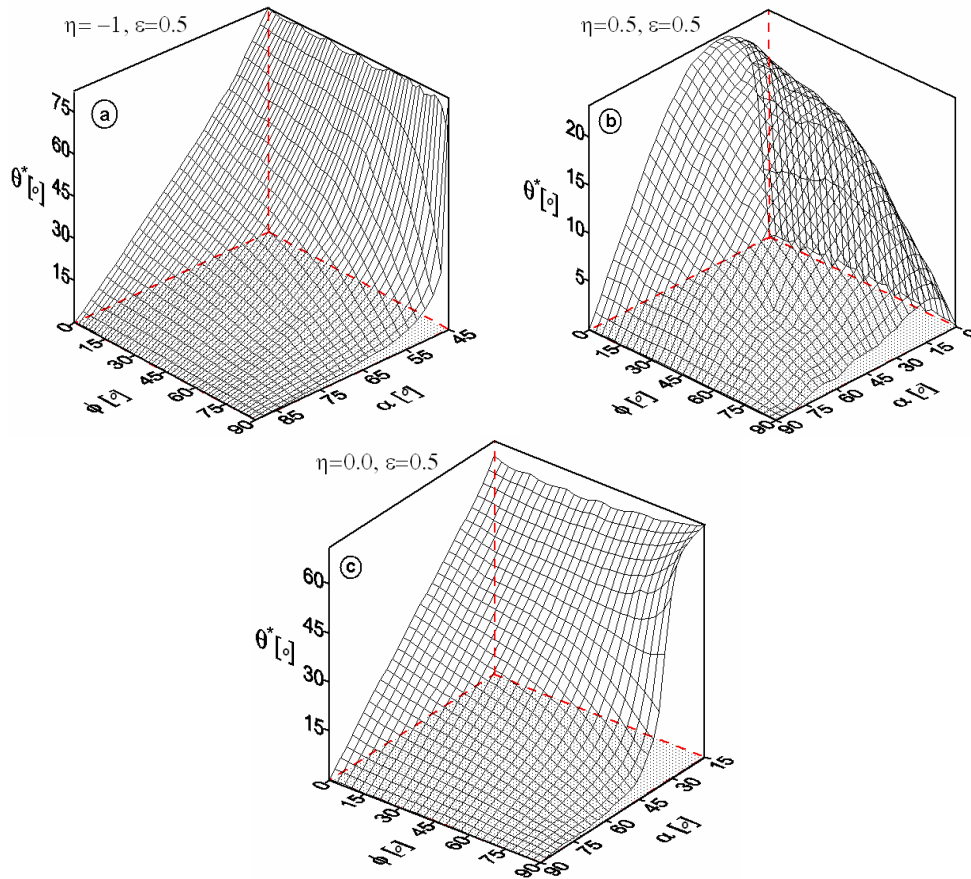


Figure 5. Crack propagation angles along inclined crack fronts.

Using the SED-criterion the crack extension angles  $\theta^*$  are plotted for the surface flaws in Fig.5 as functions of both inclination and crack front position angles for different biaxial loading conditions of semi-elliptical surface crack ( $\varepsilon=0.5$ ). As can be seen in Fig.5, the crack propagation angle  $\theta^*$  is equal to zero for all biaxial loading cases

when the initial crack is not inclined, i.e.  $\alpha=90^\circ$  represents pure mode I conditions. In this case the crack propagation angle save its value  $\theta^* = 0^\circ$  along whole curvilinear crack front. It can also be observed from Fig. 5(a) that, the crack growth angle  $\theta^*$  takes its maximum value near the free surface and decreases along the crack front towards the deepest point. It should be noted that on the free surface of plate at  $\phi = 0^\circ$  when  $\eta = -1$ ,  $\alpha=45^\circ$  take place the mixed mode II and the crack propagation angle is equal to  $\theta^* = 75^\circ$ , while for the same values of  $\eta = -1$ ,  $\alpha \approx 45^\circ$  near the deepest point of the crack front  $\phi = 90^\circ$ , the crack extension angle the sudden jump to  $\theta^* \approx 10^\circ$  take place the mixed mode III. Unlike of this situation, under uniaxial tension ( $\eta = 0$ ) the crack growth angle  $\theta^*$  can increase or decrease along the semi-elliptical crack front. As it follows from Fig. 5(c), it depends on a given inclination angle. Due to the mode mixity parameters changes along the crack front, the crack growth direction angle, must also change from point to point along the crack front. This leads in different degrees of non-planar extension along the crack front.

## CONCLUSIONS

The behavior of inclined surface semi-elliptical cracks in plate subjected to different biaxial loading is investigated. On the basis of 3D-numerical analysis the elastic-plastic stress fields depending on the crack front location, inclination crack angle, aspect ratio, crack tip distance and load biaxiality are determined. Both the elastic and plastic mode mixity parameters were introduced which are accounting for all three fracture modes to enforce of the geometrical nature of the inclined surface cracks. The mixed mode behavior of crack growth direction angle along the semi-elliptical crack front for different combination of biaxial loading, inclination crack angle and surface flaw geometry is determined. It was shown for both semi-circular and semi-elliptical crack types, that the load biaxiality has a principal effect on both the crack growth direction angle and the mode mixity parameters behavior along the crack front.

## REFERENCES

1. Sih, G.C., Chen, C. (1985) *J.Theor. Appl. Fract. Mech.* **3(2)** 125-139.
2. Dodds, R.H., Shih, C.F., Anderson, T.L. (1993) *Int. J. Fract.* **64**, 101-33.
3. Lee, M., Boothman, D.P., Luxmoore, A.R. (1999) *Int. J. Fract.* **98**, 37-54.
4. He, M.Y., Hutchinson, J.W. (2000) *Eng. Fract. Mech.* **65**, 1-14.
5. Ayhan, Ali O. (2004) *Engng. Fract. Mech.* **71**, 1079-1099.
6. Wang, X. (2006) *Eng. Fr. Mech.* **73**, 1581-1595.
7. ANSYS. Theory Reference (1999) Eleventh ed., SAS IP, Inc.
8. Sih, G.C. (1974) *Int. J. Fract.* **10 (3)**, 305-321.